Ocean Sci. J. (2014) 49(4):449-463
http://dx.doi.org/10.1007/s12601-014-0042-5

Article

Available online at http://link.springer.com

SpringerLink

Ocean Science Journal

Fragilariopsis kerguelensis Response to Iron Enrichment Regarding Its Growth, Uptake of Nutrients and Trace Metals, and Changes in CO_2, CH_4, and N_2O

Young Shin Kwon[1,2], Tae Siek Rhee[1,2]*, Sun Young Kim[1,4], Mi Seon Kim[3], Man Sik Choi[3], Eun Jin Yang[1], and Young-Nam Kim[1,5]

[1]*Division of Polar Ocean Environment, Korea Polar Research Institute, KIOST, Incheon 406-840, Korea*
[2]*Department of Polar Sciences, Korea University of Science and Technology, Daejeon 305-350, Korea*
[3]*Department of Ocean Environmental Science, College of Natural Sciences, Chungnam National University, Daejeon 305-764, Korea*
[4]*Department of Ocean Science, College of Natural Sciences, Inha University, Incheon 402-751, Korea*
[5]*Marine Ecosystem Management Team, Korea Ocean Environment Management Corporation, Seoul 135-870, Korea*

Received 19 September 2014; Revised 13 October 2014; Accepted 25 November 2014

Abstract – We performed laboratory experiments to investigate the response of *Fragilariopsis kerguelensis*, a predominant diatom species in the Southern Ocean, to different concentrations of dissolved iron in the culture medium to assess changes in nutrients, trace metals, and greenhouse gases-CO_2, CH_4, and N_2O-during growth. *F. kerguelensis* was cultured in standard f/2+Si media contained in closed chambers at 2°C, which is a typical surface temperature of the Southern Ocean in summer, under continuous irradiation with ~44 μmol photons m^{-2} s^{-1} for 8 days. The media contained 2.2 nM, 7.0 nM, and 10.6 nM of dissolved iron at inoculation. *F. kerguelensis* grew faster if the initial dissolved iron concentration was higher. Its production rate was ~40 cells mL^{-1} d^{-1} with an increase of 10^{-18} molar dissolved iron on a single cell basis. Fe and Mo were consumed faster than the growth rate at higher dissolved iron concentrations while Mn and Zn were consumed more slowly taking the mean values into account. Nitrate consumption by single cells increased with an increase of dissolved iron in the media, but phosphate and silicate showed a tendency to decrease. Hence, dissolved iron enhanced uptake of nitrate, but not the other nutrients, on a single cell basis. The carbon uptake per cell decreased with an increase in dissolved iron, which is opposite to the growth rate, suggesting that carbon content in single cells could not keep up with the cell growth. The iron efficacy of carbon uptake by single cells, defined as the ratio of the carbon uptake to the iron uptake, also showed a significant reduction with an increase in dissolved iron. This implies the inefficient usage of iron to absorb carbon at a high dissolved iron concentration. CH_4 uptake by *F. kerguelensis* occurred in our experiments, but it was trivial in relation to the overall impact. N_2O was consumed at a lower concentration of dissolved iron, but was emitted at a higher dissolved iron concentration, suggesting a facultative response of *F. kerguelensis* to the available dissolved iron.

Key words – *Fragilariopsis kerguelensis*, iron efficacy, greenhouse gases, culture experiment

*Corresponding author. E-mail: rhee@kopri.re.kr

1. Introduction

Iron is essential for the growth of marine phytoplankton. First, iron is a structural component of the enzymes required for the reduction of nitrite (or nitrate) to ammonium (Price 1994; Maldonado and Price 1996; Morel and Price 2003). Therefore, under artificially iron-depleted conditions, the uptake of nitrate and the assimilation of nitrogen of phytoplankton decline (Price 1994). Second, iron plays a crucial role in carbon assimilation in phytoplankton. A number of enzymes related to the electron transfer reactions of photosynthesis and many reductases for biochemical substances contain iron (Doucette and Harrison 1990; Geider et al. 1993; Lane and Morel 2000; Morel and Price 2003). When the iron concentration is low, the production of these enzymes declines (Geider and La Roche 1994).

A series of field experiments to investigate the effects of iron on the growth of phytoplankton, so-called FeAXs (Iron Addition Experiments) (Boyd et al. 2007), sought to find ways to lower the atmospheric carbon dioxide concentration

via the enhancement of oceanic uptake of CO_2 by intensifying the primary production of marine phytoplankton, stimulated by artificially injected dissolved iron. Physiological and ecological mechanisms of phytoplankton living in the pelagic ocean are affected by the iron concentration (Jickells et al. 2005). Primary production of half the world's oceans may suffer from a limited iron supply (Moore et al. 2001). In particular, the Southern Ocean is well-known as a high-nutrient and low-chlorophyll region where dissolved iron is one of the key limiting factors controlling primary production (Sarmiento and Orr 1991). The dissolved iron concentration was observed to be less than 0.2 nM in the Ross Sea (Fitzwater et al. 2000), 0.3-0.4 nM in the Antarctic circumpolar current (Loscher et al. 1997), and 1.2-1.9 nM in the Antarctic polar frontal zone (de Baar et al. 1995). Therefore, the organisms in the Southern Ocean should be adapted to iron-depletion. Several FeAXs experiments in the Southern Ocean revealed a dramatic increase in carbon uptake and the rapid proliferation of phytoplankton upon the injection of artificially dissolved iron (Martin 1990; Boyd et al. 2000; Buesseler et al. 2004; Coale et al. 2004; Boyd et al. 2007).

So far, fewer laboratory experiments on iron addition have been conducted than field studies, although the trend is steadily growing. Brand et al. (1983) and Sunda et al. (1991) reported that the growth rates of phytoplankton decreased when iron was scarce and that coastal species required more iron than pelagic species. Doucette and Harrison (1991) showed that only when phytoplankton growth depended on nitrate and not on ammonium as the source of nitrogen, it required a high concentration of iron. Van Leeuwe et al. (1997) found, in a series of culture experiments in Antarctic species, that a limitation of iron did not affect the composition of planktonic cells but did affect their growth rates. It was found that the intracellular production of dimethylsulfoniopropionate (DMSP), a precursor of dimethyl sulfide (DMS), was influenced by the iron concentration and the light intensity (Stefels and van Leeuwe 1998). Van Oijen et al. (2004) studied the co-limitation of iron concentration and irradiation on photosynthesis in phytoplankton by measuring the quantity of intracellular particulate organic nitrogen (PON), particulate organic carbon (POC), and polysaccharides in culture experiments. Additionally, Hoffmann et al. (2007) argued that the component ratio of silicate in diatom species decreased in Fe-replete conditions.

Despite the growing number of studies in the laboratory and at sea, few studies have focused on the impact of non-CO_2 trace gases relevant to climate change with respect to the stimulation of an ecosystem by dissolved iron (Wingenter et al. 2004; Boyd et al. 2007). We addressed here the impact of iron enrichment on changes in long-lived greenhouse gases, such as methane (CH_4) and nitrous oxide (N_2O), as well as on the key trace gas, CO_2, by means of altering the responses of phytoplankton in culture experiments conducted in the laboratory under controlled conditions. The complexities of nature were converted to a simple and controlled laboratory setting to comprehend the nature of the diatom because the interaction between marine organisms and variations in iron concentration is not a linear but rather a nonlinear phenomenon caused by many natural factors in the real world (Boyd and Ellwood 2010).

2. Material and Culture Media

We chose a diatom species, *F. kerguelensis*, for this study. It is one of the most predominant plankton species in the water column and sediment of the Southern Ocean and plays a key role in the Antarctic pelagic ecosystem (van der Spoel et al. 1973; Zielinski and Gersonde 1997; Smetacek et al. 2004).

Pre-incubation

An aliquot of *F. kerguelensis* was incubated in a standard f/2+Si medium (Guillard 1975) before inoculation into culture containers. The medium was treated to remove all trace metals by passing it through a Nobias-chelate PA1 resin and sterilized by autoclaving at 121°C. *F. kerguelensis*, however, hardly grew in this medium because of a lack of dissolved iron. The addition of trace metals required for the standard f/2+Si medium caused *F. kerguelensis* to thrive in a short period of time. However, this addition prevented us from working with an iron-free medium because the medium contained iron, which was carried over to the culture media.

Culture media

Seawater collected onboard R/V *Araon* in the Southern Ocean (63.59°S, 107.45°W) in December, 2010, was used for this culture experiment. Before *F. kerguelensis* was inoculated, the seawater was filtered through a GF/F filter (0.45 μm) and a polycarbonate (PC) membrane filter (0.2 μm) to remove all organisms, including bacteria, and was then sterilized in an autoclave at 121°C. A portion of the seawater was used as a control medium (0Fe), and the remainder was further treated with Nobias-chelate PA1 resin to remove

trace metals. The resin column and its container had been thoroughly cleaned and washed with nitric acid, hydrochloric acid, acetone, and hydrofluoric acid to remove any trace metals before treatment of the seawater. The seawater was filtered once more through a PC membrane filter to ensure that there were no particulate materials in the seawater medium after the removal of trace metals. An iron-limited medium (-Fe) was prepared by adding major nutrients (phosphate, nitrate, and silicate), vitamins, and trace metals, except iron, to the seawater according to the recipe for the f/2+Si medium (Guillard 1975). Despite careful treatment of the seawater media during preparation to prevent iron contamination, the -Fe medium contained 2.2 nM of dissolved iron from the iron added to the pre-cultured medium that was carried over to the seawater. An iron-replete medium (+Fe) was prepared by adding $FeCl_3$, resulting in 10.6 nM of dissolved iron. The seawater media was thoroughly mixed for 3 days with nutrients, vitamins, and trace metals added. The initial conditions of the culture media are listed in Table 1.

Inoculation and the closed culture system

Pre-incubated *F. kerguelensis* was inoculated into 1.8 L of seawater media contained in three 4.5 L polypropylene containers. The headspace of the containers was partially flushed with ultra-pure nitrogen (99.9999%) immediately after inoculation and remained closed in the course of the experiments. The containers were shaken and placed in a culture room for one day until equilibrium of the trace gases between the headspace and the seawater media was reached before collecting samples.

During the entire duration of the experiment, the containers were in a culture room at 2℃ under fluorescence lamp (44 μmol photons m^{-2} s^{-1}) for 24 hours per day under closed conditions.

3. Methods

Sampling

To monitor the growth of *F. kerguelensis*, 10 mL of seawater was sampled from each container at an interval of 1-2 days. Before sampling, the same volume of ultra-pure N_2 (99.9999%) as the sample being collected was injected into the container to maintain the internal pressure of the container. Dissolved trace metals and nutrients in the culture media were analyzed by collecting 100 or 110 mL of samples, and CO_2, CH_4, and N_2O concentrations in the headspace were analyzed by collecting a 90 mL air sample. To maintain the internal pressure, the total volume of headspace or seawater collected, e.g. 190 or 200 mL, was replaced with ultra-pure N_2 (99.9999%).

Cell counting

Of the 10 mL seawater sample, 2 mL was used to measure *in-vivo* fluorescence with Trilogy and the remainder was fixed with glutaraldehyde (final concentration 1%). The fixed seawater (1-5 mL) was filtered with a PC membrane filter (0.2 μm), which was then dyed with DAPI to count the number of phytoplankton using a microscope.

Nutrients

Nitrate (NO_3^-), phosphate (PO_4^{3-}), and silicate ($Si(OH)_4$) were analyzed by a typical colorimetric method using an auto-analyzer (AACS V, Japan). The automated analytical system was calibrated with a reference material (Moss nutrient, U.S.A.). The regression coefficients of the calibration curves were always higher than 0.9999.

Trace metals

Trace metals were analyzed via Inductively Coupled Plasma Mass Spectrometry (ICP-MS; X-7 model, Thermo Finnigan Ltd.) following the preparation technique described by Sohrin et al. (2008). In brief, the pH of an aliquot of seawater was adjusted to pH 6 by adding ammonium acetate ($NH_4C_2H_3O_2$). The seawater was then loaded onto Nobias-chelate PA1 resin at 3 mL min^{-1} to concentrate the trace metals. The remaining salt in the resin was washed out with 10 mL of 2% ammonium acetate. The trace metals concentrated in the resin were eluted by adding 5 mL of 1 M HNO_3. This concentrate was analyzed by ICP-MS. Certified reference materials (CASS-5 and NASS-5) were analyzed to verify the analytical method (Table 2). Dissolved iron (DFe) was recovered within

Table 1. Initial conditions of culture media

Media ID	Cell density (mL^{-1})	Nitrate (μM)	Phosphate (μM)	Silicate (μM)	Fe (nM)	Mn (nM)	Mo (nM)	Zn (nM)	CO_2 (ppm)	CH_4 (ppb)	N_2O (ppb)
-Fe	12500 ± 1100	964 ± 39	20 ± 1	166 ± 7	2.2 ± 0.1	307 ± 12	28 ± 1	7.3 ± 0.3	105 ± 4	376 ± 15	53 ± 2
0Fe	17500 ± 3900	65 ± 3	18 ± 1	105 ± 4	7.0 ± 0.3	382 ± 15	96 ± 4	28 ± 1	173 ± 7	596 ± 24	70 ± 3
+Fe	18900 ± 3700	1012 ± 40	22 ± 1	155 ± 6	10.6 ± 0.4	290 ± 12	28 ± 1	11 ± 0.4	175 ± 7	684 ± 27	95 ± 4

Table 2. Validation of trace metal analyses using certified reference materials of CASS-5 and NASS-6 from National Research Council of Canada

CRM		Fe (μg kg^{-1})	Mn (μg kg^{-1})	Zn (μg kg^{-1})
CASS-5	Certified	1.40 ± 0.11	2.56 ± 0.20	0.702 ± 0.067
	Analyzed	1.41 ± 0.02	2.76 ± 0.04	0.507 ± 0.037
	Recovery (%)	101 ± 8	108 ± 9	72 ± 9
NASS-6	Certified	0.483 ± 0.045	0.516 ± 0.047	0.251 ± 0.020
	Analyzed	0.525 ± 0.013	0.604 ± 0.017	0.111 ± 0.017
	Recovery (%)	109 ± 11	117 ± 11	44 ± 8

analytical uncertainty, whereas dissolved Mn was slightly larger than the certified values and dissolved Zn was less than the certified values.

Greenhouse gases

N_2O and CH_4 in the headspace of the containers were analyzed with an automated HP5890 gas chromatographic system (Rhee et al. 2009). CH_4 was separated by a packed Carboxen 1000 column at 60°C with N_2 (99.9999%) as the carrier gas flowing at 40 mL min^{-1}, and N_2O was separated by a Porapak Q column at 35 mL min^{-1} using the same carrier gas at the same temperature. After separation, N_2O and CH_4 were detected by an electron capture detector (ECD) and a flame ionization detector (FID), respectively. CO_2 concentration was determined by injecting 50 mL of the headspace air into the cell of a Li-6262 CO_2/H_2O Analyzer (LI-COR Biosciences). Both analytical systems were calibrated with standard gases traceable to the NOAA scale.

As mentioned in section 3.1. Sampling, the headspace air or seawater collected for analyses was replaced with the same volume of ultra-pure N_2. This "dilution" effect must be corrected for. The dilution factor (F_a) due to the replacement of the headspace air can be described as the ratio of the headspace volume before and after sample collection:

$$F_a = \frac{V_h}{V_h - V_a} \quad (1)$$

where V_h indicates the volume of the headspace in the container when collecting the air sample and V_a the volume of the air sample collected. An additional correction for collecting the water sample in the container should be performed because the same volume of N_2 gas was replaced. This can be done by adding the volume of the seawater collected, V_w, to the headspace since the headspace expanded:

$$F_w = \frac{V_h + V_w}{V_h} \quad (2)$$

Combining (1) and (2),

$$F = \frac{V_h + V_w}{V_h - V_a} \quad (3)$$

Taking dilution into account, the absolute amount of gas i in the headspace, n_{ia}, is:

$$n_{ia} = m_{ia} \times \frac{V_h}{v_m} \times F^{n-1} \quad (4)$$

where m_{ia} indicates the mole fraction of gas i in the headspace, v_m the molar volume of the air in the headspace at the experimental temperature (22.578 L mol^{-1} at 2°C), and n the number of collections of the headspace air before sampling.

The absolute amount of gas i dissolved in the seawater can be obtained by Henry's law, assuming that gas i was always in thermodynamic equilibrium between the headspace and seawater:

$$n_{iw} = m_{ia} \times (P - P_H) \times K_i \times V_s \times G_i \quad (5)$$

where P indicates the internal pressure of the container, P_H vapor pressure, K_i Henry's law constant of gas i at a given temperature, V_s volume of the seawater in the container before collection of air, and G_i the dilution factor due to the reduction of the seawater. Because the container was a closed system, we took the sum of the absolute amount of gas i in the headspace and the seawater into account to examine the biological effect on greenhouse gases.

$$n_i = n_{ia} + n_{iw} \quad (6)$$

For CO_2, we calculated dissolved inorganic carbon (DIC) in the seawater as dissolved CO_2 ($CO_2(aq)$), carbonic acid (H_2CO_3), and bicarbonate (HCO_3^-) and carbonate (CO_3^{2-}) ions formed in thermodynamic equilibrium between the dissolved CO_2 and the ionic species.

$$DIC = [CO_2(aq)] + [H_2CO_3] + [HCO_3^-] + [CO_3^{2-}] \quad (7)$$

Total alkalinity (TA) was determined using the pH (= 8.0) of

the seawater and the CO_2 concentration in the headspace measured right before the start of the experiment, assuming thermodynamic equilibrium of the CO_2 between the headspace and the seawater media. Because TA is not altered by the change in CO_2 in the culture container, DIC can be calculated using the CO_2 concentration in the headspace during the experiments.

Leakage of the container was thoroughly examined before and after the experiments by measuring the CH_4, N_2O, and CO_2 concentrations in the empty container by adding enough N_2 gas for these gas concentrations to be lower than those in the ambient air. CH_4 was slightly increased at 4.3 ppb d^{-1}, while N_2O and CO_2 were not detectable. We accounted for the increased rate of CH_4 in the final results of the culture experiments.

4. Results and Discussion

Growth rate of the diatom

All culture experiments showed an exponential increase in cell density of the diatom (Fig. 1). Because the culture experiments were conducted without a grazer, we adopted a simple exponential growth of phytoplankton to determine the growth rate, μ (Hoogenhout and Amesz 1965; Laws 2013):

$$N_t = N_0 e^{\mu t} \quad (8)$$

where N_0 and N_t indicate the cell density at the initial time and a given time, respectively. The growth rates of *F. kerguelensis* in -Fe, 0Fe, and +Fe media were 0.130(±0.038) d^{-1}, 0.219(± 0.017) d^{-1}, and 0.183(± 0.029) d^{-1}, respectively (Fig. 2). DFe seems to have stimulated the growth of *F. kerguelensis*, as the growth rate was enhanced with an increase in the initial DFe. An exception is the case of 0Fe, where the diatoms grew faster than in +Fe despite the smaller initial DFe value. The difference between 0Fe and the other media is the presence or absence of EDTA and f/2+Si trace metal stock solution in the culture medium. In general, EDTA in the medium buffers DFe by preventing dissolved ferric ions from precipitating in the media. However, adding EDTA appeared to suppress the growth of *F. kerguelensis* in this experiment. Hoffmann et al. (2007) also reported the same results from culture experiments with *F. kerguelensis* with and without the addition of EDTA such that the growth rate decreased with added EDTA. These two experiments directly indicate that added EDTA either may mask the DFe such that the apparent DFe would be larger than the biologically available amount, most likely due to the high affinity of the ferric ion to EDTA, which mimics natural organic ligands (Gerringa et al. 2000), or could have a negative effect because of the photo-reduction of complex ferric ions to ferrous ion (Lewin and Chen 1971; Anderson and Morel 1982).

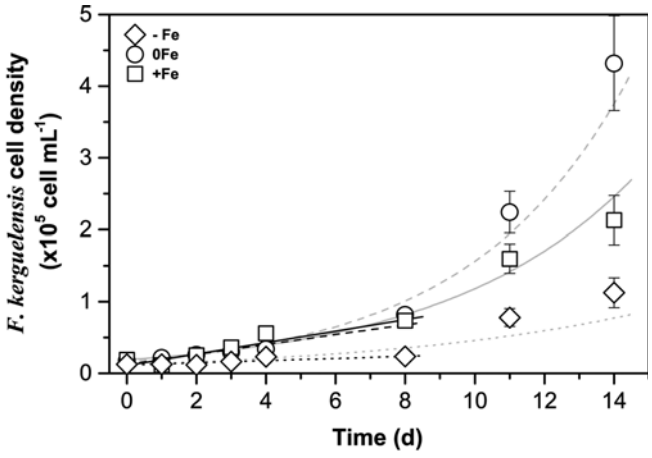

Fig. 1. Exponential increase in cell density of *F. kerguelensis* during the culture experiments under different conditions

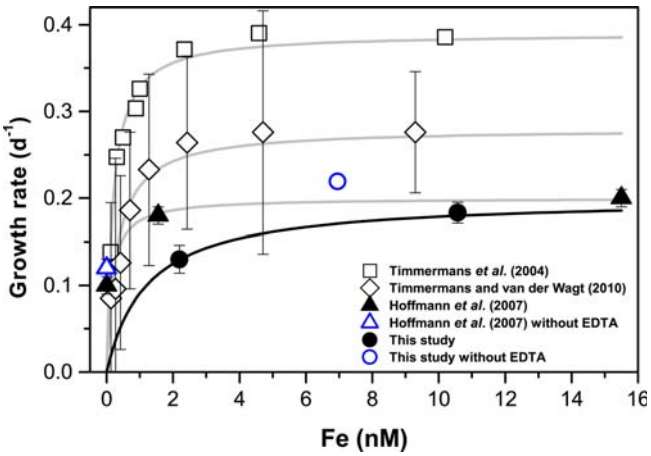

Fig. 2. Growth rate as a function of the limiting parameter, dissolved iron, with the Monod fitting to determine the half-saturation constant, K_m, and maximum growth rate, μ_{max}. For the sake of comparison, the results from Timmermans et al. (2004), Timmermans and van der Wagt (2010), and Hoffmann et al. (2007) are shown as they performed similar laboratory experiments with *F. kerguelensis*

Applying Monod's growth model (Monod 1949) with the initial DFe as the limiting factor produces the half-saturation value K_m and the maximum growth rate μ_{max} of 1.27 nM and 0.21 d^{-1}, respectively (Fig. 2). Hoffmann et al. (2007) observed a similar μ_{max} from their culture experiments

in the laboratory with added EDTA. In their experiments, *F. kerguelensis* grew 0.18 d^{-1} and 0.20 d^{-1} at 1.55 nM and 15 nM DFe, respectively, while its growth rate decreased by as much as approximately twice to 0.10 ± 0.01 d^{-1} in an iron-free medium. According to the Monod model, K_m is, however, approximately 10 times lower than the value obtained in our experiments. We suspect that the cell density in the culture media might be the reason that the K_m values are different between the two experiments, although Hoffmann et al. (2007) did not describe the cell density but the Chlorophyll-a concentration as a surrogate. Timmermans et al. (2004) and Timmermans and van der Wagt (2010) also determined K_m to be in the range of 0.2-0.3 nM, which is also far smaller than the value we obtained, and μ_{max} to be 0.4 d^{-1}, which is approximately twice as large as the growth rate from Hoffmann et al. (2007) and our experiments (Fig. 2). Our lower value could be due to the density of the diatoms in the media; while the initial density of *F. kerguelensis* in a study by Timmermans et al. (2004) was ~200 cells mL^{-1}, ours was > ~12000 cells mL^{-1} (Table 1). Thus, in the following sections concerning temporal variation of the substrate in the culture medium, we will use normalized DFe (NDFe) values with respect to the initial cell number in the media rather than the total amount of DFe.

As mentioned above, the half-saturation constant, K_m, was 1.27 nM in our experiments, which implies that DFe would not act as a limiting factor in a range of DFe values larger than 3.4 nM (*e*-folding factor). The growth rates obtained in our experiment reflect that it took between 3.1 and 5.3 days to double the number of the diatom cells. The exponential increase in the number of cells in equation (8) can be simplified to a linear fit as the higher than 2nd order polynomial diminishes in the Taylor expansion.

$$e^{\mu t} = 1 + \mu t + \frac{\mu^2}{2} t^2 + \cdots \quad (9)$$

$$1 + \mu t >> \frac{\mu^2}{2} t^2 + \cdots \quad (10)$$

Solving equation (10), neglecting the higher than 2nd order polynomials, the maximal time span, t_{max}, during which linear growth is valid is

$$t_{max} = \frac{1 + \sqrt{3}}{\mu} \quad (11)$$

, which yields a t_{max} between 12 and 21 days for our experiments. Therefore, we may safely assume that the number of diatom cells grew in a linear manner for the first 8 days, as it is shorter than the calculated t_{max}.

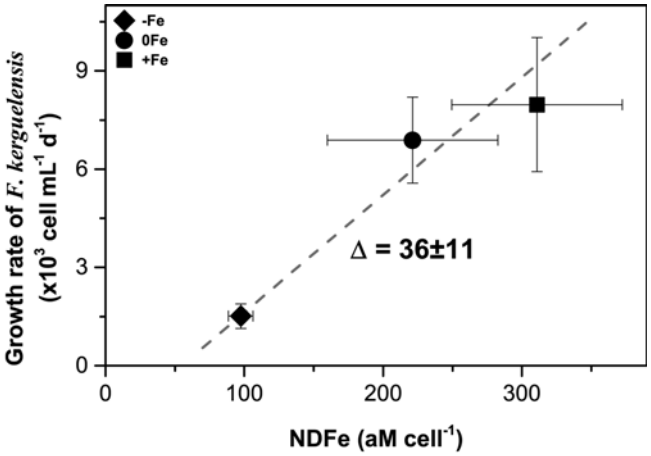

Fig. 3. Comparison of the linear growth rate for 8 days of culture period against the initial dissolved iron concentration normalized with cell numbers (NDFe). The linear growth rate fitted to the data is shown in Fig. 1

Applying a linear growth fit to the measurements up to 8 days, the linear growth rate is augmented with the initial NDFe increase, although the growth rate in 0Fe medium without added EDTA is a little higher than the growth rate obtained in -Fe and +Fe media when EDTA was added (Fig. 3), indicating an adverse effect of EDTA. The linear growth rate of *F. kerguelensis* shows an increasing tendency with an NDFe of 36(±11) cell mL^{-1} d^{-1} (aM Fe $cell^{-1})^{-1}$ (Fig. 3), suggesting that iron is a critical ingredient for the growth of *F. kerguelensis*.

Nutrients

Temporal trends for the major nutrients-nitrate, phosphate, and silicate-were determined based on the experimental results obtained during the 8-day linear growth period (Fig. 4a-4c). The nutrients in the +Fe medium decreased, with nitrate showing the largest uptake rate of -14(± 14) μM d^{-1}, followed by silicate at -2.7(± 0.5) μM d^{-1} and phosphate at -0.11(± 0.06) μM d^{-1}. In 0Fe and -Fe media, temporal variations of the nutrients did not show as clear a trend as was seen in the +Fe medium.

Because nutrients in the culture media change depending on the degree of biological activity and the cell density, the temporal variation was normalized with the linear growth rate of *F. kerguelensis* (Fig. 4d-4f). The nitrate uptake rate normalized to the cell growth seemingly shows an increasing tendency with an increase of NDFe, although a large degree of uncertainty does not allow statistical confidence (Fig. 4d). It was demonstrated in the laboratory experiments that

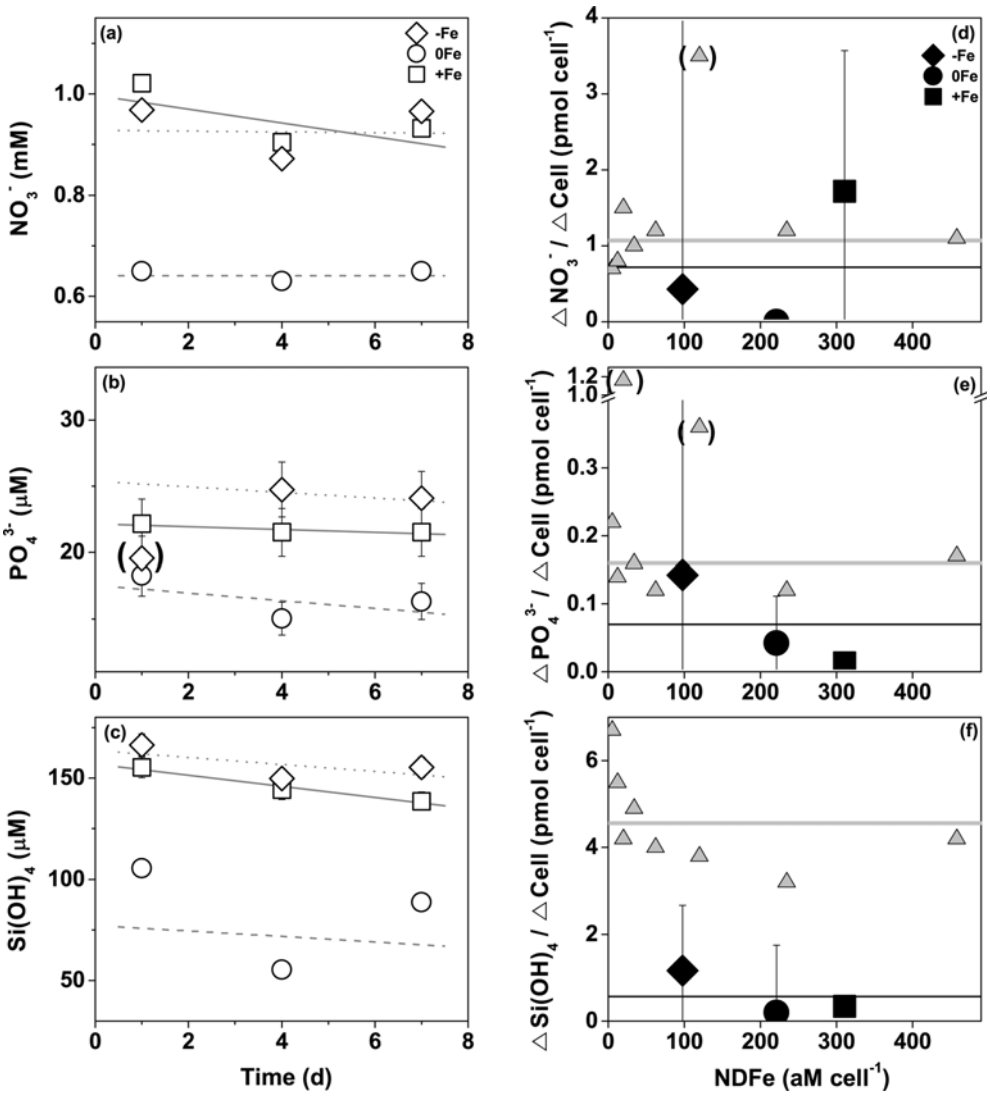

Fig. 4. Temporal variations of (a) nitrate, (b) phosphate, and (c) silicate in the culture media and the consumption rates by single cells against the initial dissolved ion concentration normalized with cell numbers (NDFe) for (d) nitrate, (e) phosphate, and (f) silicate. Nitrate concentrations in the 0Fe medium in (a) should be read by multiplying by a factor of 10. The datum at day 1, marked with parentheses, was excluded when determining the uptake rate of phosphate in the -Fe medium. Consumption rates by single cells of *F. kerguelensis* from Timmermans et al. (2004) are plotted for comparison (triangle symbol). Note that NDFe in the media by Timmermans et al. (2004) should be read by multiplying by a factor of 1000. Timmermans et al. (2004) provided dissolved iron concentrations, not NDFe, which was computed provided that the cell density was 200 cells mL^{-1} and the volume of the culture media was 100 mL. The gray line indicates the mean value for Timmermans et al. (2004), excluding the value marked with parentheses, and the black line is the mean value of the results from this experiment

dissolved iron stimulates the enzymatic activation of nitrate reduction and thus uptake of nitrate (Maldonado and Price 1996; Price et al. 1994), which could explain our observation. The average of three values was 0.72(± 4.31) pmol cell^{-1}. Timmermans et al. (2004) did a series of experiments at different DFe levels showing that the increasing tendency occurred in the range of low concentrations (< ~20 fM cell^{-1}) and that the uptake rates were almost invariable beyond that (Fig. 4d). Note that the DFe values for Timmermans et al. (2004) were computed provided that the cell density was 200 cells mL^{-1} and the volume of the culture medium was 100 mL, which yields a ~1000-fold larger NDFe than that in our work. Their mean value of nitrate consumption rate per cell is 1.07 pmol cell^{-1} which is ~1.5-fold larger than the mean value from our experiments, but which is the same magnitude in the range of uncertainties.

Phosphate in the media did not vary significantly regardless of the DFe concentration. However, ignoring the large uncertainties at low values of NDFe, the mean uptake rate per cell seemingly slowed down with an increase of NDFe (Fig. 4e). A similar downward trend could be found in the range of low concentrations of NDFe for Timmermans et al. (2004), although their uptake rates per cell are far larger than ours considering their NDFe. The overall mean value of 0.16 pmol cell^{-1} is 2.4-fold larger than ours.

Because the frustules of diatoms are composed of polymerized silicic acid, the diatoms should consume silicate proportionally during growth. The silicate uptake rate normalized to the cell growth was 0.64(± 0.84), 0.11(± 0.86), and 0.19(± 0.06) pmol cell^{-1} for -Fe, 0Fe, and +Fe, respectively (Fig. 4f). This indicates that a lower dissolved iron concentration in the seawater enhanced the uptake rate of silicate more greatly for each cell. Such an enhancement of the silicate uptake with reduced DFe in seawater has been observed in other experiments (Timmermans et al. 2004; Hoffmann et al. 2007; Timmermans and van der Wagt 2010). As shown in Fig. 4f, the silicate consumption rate exponentially decreases from ~7 pmol cell^{-1} to 3 pmol cell^{-1} according to Timmermans et al. (2004). Such a decreasing tendency of silicate uptake rate with increasing NDFe is most likely due to the efficient uptake of dissolved iron and silicate at lower levels of DFe (Sunda and Huntsman 1995; Timmermans and van der Wagt 2010). Apart from a similar trend in NDFe, the mean consumption rates per cell were far different: the overall mean value of 4.6 pmol cell^{-1} for Timmermans et al. (2004) was 8-fold larger than ours. Although it is not certain what caused the nutrient uptake rates per cell in our experiments to be lower than those in Timmermans et al. (2004), the huge difference in NDFe and the cell density probably play a role.

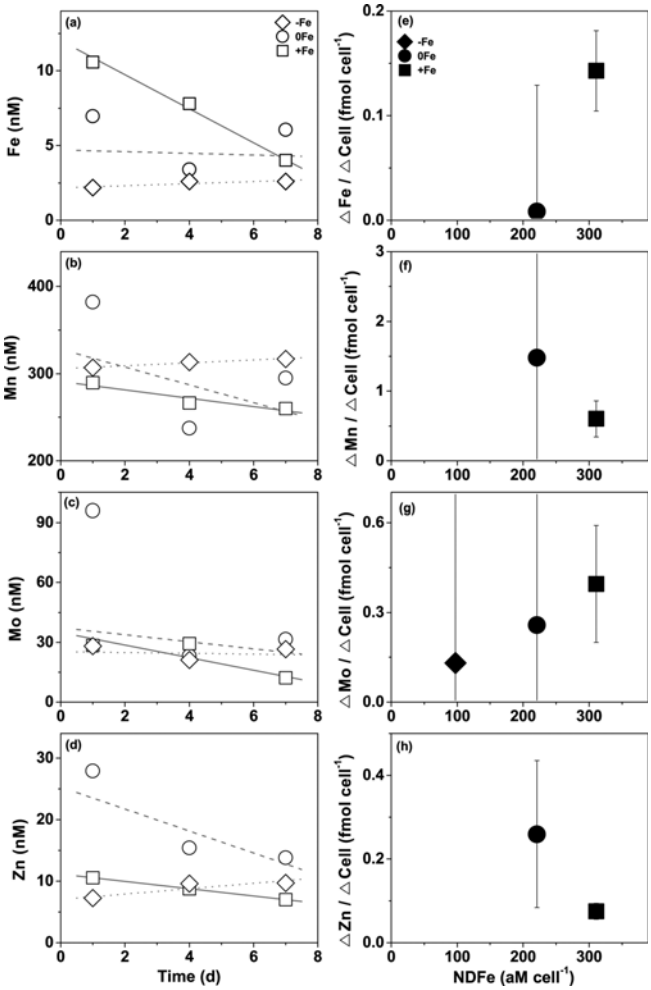

Fig. 5. The same as Fig. 4 but for trace metals. (a) and (e) dissolved Fe, (b) and (f) dissolved Mn, (c) and (g) dissolved Mo, and (d) and (h) dissolved Zn

Trace metals

Among the trace metals detected by ICP-MS, Fe, Mn, Mo, and Zn dissolved in the seawater media were greater than ~1 nM, which was reliable and far larger than the detection limit. Thus, we focused on temporal variations of these trace metals associated with the growth of *F. kerguelensis*.

The uptake rate of dissolved Fe followed the NDFe in the media; 0.07(± 0.04) nM d^{-1}, 0.06(± 0.83) nM d^{-1}, and -1.14(± 0.09) nM d^{-1} in the -Fe, 0Fe, and +Fe media, respectively (Fig. 5a). Normalized with the linear growth rate, *F. kerguelensis* consumed DFe more rapidly in the +Fe medium than in the others, which is similar to the luxury uptake of DFe by phytoplankton often observed in laboratory experiments (Sunda and Huntsman 1995; Marchetti et al. 2006; Marchetti et al. 2010). Van Leeuwe et al. (1997) found that DFe absorbed by *F. kerguelensis* was threefold larger in the medium with an initial DFe of 10 nM compared to 2 nM, which indicates that the absorption rate of DFe is proportional to the DFe concentration in the medium.

Dissolved iron exists in various speciations in the media. Among these, phytoplankton absorb only inorganic species, which ends up with conversion to Fe^{2+} on cell surfaces due to the enzymatic reduction of ferric ion complexes that are delivered bound to an organic ligand (Rue and Bruland 1995; Hassler et al. 2011). We estimated the fraction of Fe^{3+} that exists as inorganic complexes, organic ligands, and a bound form with EDTA using the stability constants of iron

complexation chemistry (Millero et al. 1995; Millero 1998; Gerringa et al. 2000). A simple model described in Appendix A indicates that approximately 1.5% of DFe would exist in an inorganic form and the remainder would be chelated with organic compounds and EDTA, assuming that the organic ligand concentration is ~0.17 nM (Millero 1998). This is rather large compared to the value of ~0.1% estimated in the literature (Timmermans et al. 2001; Ho et al. 2003). However, increasing the organic ligand concentrations to ~12 nM, the concentration observed in the Southern Ocean (Nolting et al. 1998), the inorganic fraction of DFe would drop to ~0.03%. Because the current technique allows us to measure the fraction of organically bound DFe, it is desirable to measure DFe speciation in future studies.

Mn, Mo, and Zn are important trace metals in the metabolism of phytoplankton (Morel and Price 2003; Twining and Baines 2013). In particular, Mo is a crucial component for nitrogen reductase to reduce nitrate to ammonium or for nitrogenase to fix molecular nitrogen (Howarth and Cole 1985). An uptake tendency was clearly observed for these trace metals in the +Fe medium, while such a tendency was not evident in the other media most likely due to the inactive biological uptake of trace metals. Uptake rates in the +Fe medium were -4.8(± 1.6) nM d^{-1}, -3.2(± 1.3) nM d^{-1}, and -0.6(± 0.0) nM d^{-1} for Mn, Mo, and Zn, respectively (Fig. 5). Compared with Fe, the uptake rates for Mn and Mo were approximately 4.2 and 2.8 times larger, which might be due to larger initial concentrations than that for DFe. If the uptake rates of the trace metals are associated with the initial concentration, the luxury uptake hypothesis is applicable to the trace metals that are critical to algal growth. It is evident that the uptake rates of these trace metals normalized with the growth rates indicate an increasing trend with an increase in NDFe, although large uncertainties in 0Fe and -Fe do not allow for a clear conclusion. Despite the large degree of uncertainty, the increasing tendency of the Mo consumption rate per cell with an increase in NDFe, which is similar to that for Fe, suggests that *F. kerguelensis* consume more nitrate at a higher NDFe. This is often observed in in-situ field experiments (de Baar et al. 2005; Hiscock and Millero 2005; Howarth and Cole 1985).

Greenhouse gases

The uptake rate of inorganic carbon was enhanced by the increase of initial DFe: -8.8(± 1.8) μM d^{-1}, -10.3(± 1.7) μM d^{-1}, and -21.4(± 6.7) μM d^{-1} in the -Fe, 0Fe, and +Fe media, respectively (Fig. 6a). However, normalization with the cell growth rate against NDFe reveals a decreasing tendency (Fig. 6d), which implies that dissolved iron stimulates the growth rate but that the amount of carbon consumed by single diatom cells was not proportional to the increase in cell numbers. The same situation has been observed for silicate; its uptake rate per cell decreased with NDFe (see Fig. 4f). The mean uptake rate of DIC by single growing cells in three different media was 3.3 pmol $cell^{-1}$, with a range of 1.5-5.8 pmol $cell^{-1}$. To our knowledge, no laboratory experiments have yet been performed to investigate the carbon consumption rate of diatoms, but the carbon quotas of the cells in different DFe media have been studied. Hoffmann et al. (2007) found that the carbon quotas of *F. kerguelensis* grown in iron-free medium were not significantly different from the medium containing 15.5 nM DFe, taking the experimental uncertainties into account. Nevertheless the mean carbon quota of 18 pmol $cell^{-1}$ is approximately 6-fold higher than the mean carbon uptake rate by single cells observed in our experiments. This should be resolved in future studies.

We monitored the temporal evolution of CH_4 in the cultures of *F. kerguelensis* for the first time (Fig. 6b). Although a slight tendency for uptake was detected in all culture media, -0.32(± 0.98) nM d^{-1} in -Fe, -0.46(± 0.17) nM d^{-1} in 0Fe, and -0.5(± 1.7) nM d^{-1} in +Fe, these values are small enough to be negligible considering their uncertainties. Although CH_4 is known to be produced or consumed during microbial activity in the marine environment, algal production of CH_4 was recently observed in micro-algal cultures in outdoor pond experiments (Florez-Leiva et al. 2010; Ferrón et al. 2012). Our laboratory experiment, however, does not indicate algal production, but consumption of CH_4. The mean uptake rate of CH_4 per cell in three different media was 0.1(± 0.2) fmol $cell^{-1}$ (Fig. 6e), which is ~30 000 times lower than the carbon uptake. Thus, even if *F. kerguelensis* consumed CH_4 and the global warming potential of CH_4 in the time horizon of 20 years (=84; Myhre et al. (2013)) is considered, its impact on the global climate is negligible (~0.3% of CO_2). However, considering the oceanic source strength of CH_4 in the Southern Ocean, the ~0.1 fmol $cell^{-1}$ of CH_4 uptake by *F. kerguelensis* is not trivial. The ratio of the uptake rate of CO_2 to CH_4 in the Southern Ocean was approximately 56 000 (Rhee et al. 2014), which is comparable to the mean uptake ratio of $\Delta CO_2/\Delta CH_4$ by *F. kerguelensis*. Although the laboratory experimental results cannot be directly compared to those from field

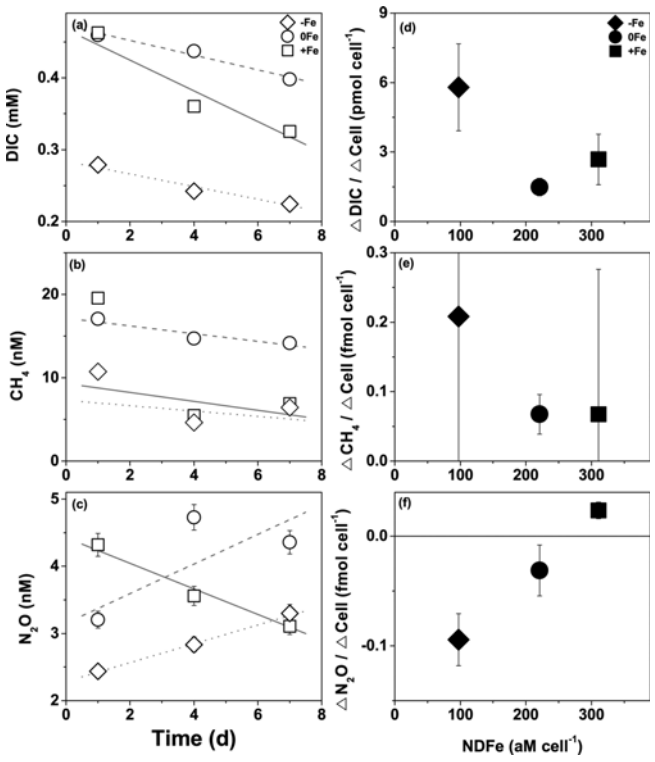

Fig. 6. The same as Fig. 4 but for greenhouse gases. (a) and (d) DIC converted from the CO_2 in the headspace, (b) and (e) CH_4, and (c) and (f) N_2O

measurements, this indicates that further study on the impact of diatoms on the budget of greenhouse gases is necessary.

Nitrous oxide (N_2O) distribution in the marine environments is mostly driven by the microbial activities of nitrification or denitrification in the water column where dissolved oxygen is limited (Elkins et al. 1978). As for CH_4, the algal production of N_2O was detected in several controlled experiments (Florez-Leiva et al. 2010; Ferrón et al. 2012). Our experiments showed that N_2O was produced at 0.14(± 0.01) nM d^{-1} and 0.22(± 0.15) nM d^{-1} in -Fe and 0Fe media, respectively, and consumed at -0.19(± 0.01) in +Fe medium, which indicates that not only the production of N_2O occurred in the culture media but that consumption also occurred in the high initial DFe medium, +Fe (Fig. 6c and 6f). We carefully investigated bacterial growth and confirmed that proliferation was negligible during the experimental period. To our knowledge, this is the first experimental result showing the production and consumption of N_2O by *F. kerguelensis*. Because our experiment was not designed to investigate the mechanism by which *F. kerguelensis* produced or consumed N_2O in the water column, we cannot suggest a potential mechanism. However, we speculate that this might be related to enhanced nitrate reduction driven by the increment of DFe in the media, which has been observed in laboratory experiments with denitrifying bacteria (Granger and Ward 2003). One hypothesis is that N_2O is produced under limited DFe conditions due to limited nitrous oxide reduction enzymes, while N_2O is preferentially taken up by *F. kerguelensis* due to the activation of N_2O reduction enzymes at high DFe concentrations. Because this is the first experimental result, further experiments are necessary to confirm the facultative mechanism of N_2O metabolism by *F. kerguelensis*.

Taking the indicated values of N_2O production or consumption by single cells into account, *F. kerguelensis* would produce N_2O ~60 000 times or consume it ~110 000 times lower than the corresponding carbon uptake rates based on the results of the present experiments. Converting this into CO_2 equivalents by multiplying by the global warming potential of 298 in the time horizon of 100 years (Myhre et al. 2013), the amount of N_2O produced or consumed by *F. kerguelensis* is as little as ~0.5% and ~0.25% of the carbon consumed, respectively. Therefore, our finding implies that production or consumption of N_2O by *F. kerguelensis*, depending on DFe concentration, would not influence the global climate. Even in terms of oceanic source or sink strength, its impact would be very minimal, taking the ratio of CO_2 uptake to the N_2O outgassing of ~1300 in the Southern Ocean into account (Rhee et al. 2014).

Synthesis

Dissolved iron stimulates the growth of *F. kerguelensis*, as shown, because the growth rate and the linear growth rate were enhanced with an increase of DFe in the initial stage (Fig. 1). While growing, they consumed nutrients, including inorganic carbon and trace metals. Whether the ratio of the consumption rates for these substrates depends on the content of DFe is a subject of debate about changes in the ecosystem due to iron fertilization (Takeda 1998; Hiscock and Millero 2005). As discussed above, our experiments did not show clear tendencies for all components with respect to the variation of DFe in the media. For instance, the trace metals show near constant or slight increasing trends in the -Fe medium. Thus, we chose mean values and the values of the +Fe medium for the uptake rates of the nutrients and trace metals by single cells to see how the DFe enrichment changed the uptake ratios of the dissolved substances in the media (Table 3). The former is indicated by the ratio of $\Delta C:\Delta N:\Delta P:\Delta Si = 50:10:1:9$, the latter by $\Delta C:\Delta N:\Delta P:\Delta Si = 200:130:1:26$. Although there are large

Table 3. Nutrients consumption ratios per iron, and Redfield and Brzezinski ratios on average and at +Fe medium

	DIC	NO^{3-}	PO_4^{3-}	$Si(OH)_4$	Fe
Fe efficacy					
Average	44000(± 46000)	9500(± 58000)	870(± 1400)	7500(± 11000)	1(± 1)
+Fe	19000(± 9000)	12000(± 13000)	90(± 60)	2400(± 1000)	1(± 0.4)
Redfield and Brzezinski ratio					
Average	50(± 70)	10(± 70)	1(± 2)	9(± 16)	
+Fe	200(± 150)	130(± 160)	1(± 1)	26(± 18)	

uncertainties in the ratios (Table 3), these two ratios imply several things about the physiology of *F. kerguelensis*. First, the ratio does not abide by Redfield (Redfield et al. 1960) and Brzezinski's (Brzezinski 1985) (RB) ratio of ΔC:ΔN:ΔP:ΔSi ≈ 106:16:1:14. Second, *F. kerguelensis* takes up carbon, nitrogen, and silicon differentially depending on the concentration of DFe. The mean ratios for these elements are lower than the RB ratio with respect to P, while in the +Fe medium, the consumption of these elements relative to P is greater than the RB ratio due to the small uptake of phosphate in the +Fe medium.

Nevertheless, enhanced uptake of NO_3^- in the +Fe medium compared to other nutrients was evident in the uptake rate by single cells (see Fig. 4d) and in the decrease of ΔC:ΔN from 4.6 to 1.6. Preferential consumption of NO_3^- by *F. kerguelensis* in the medium with increasing DFe has also been observed (Timmermans et al. 2004). The authors also reported a slight tendency of the ratio of Si to P to decrease with an increase of DFe, which could not be observed in our experiments due to the low uptake rate of PO_4^{3-} in the +Fe medium. However, a decreasing tendency of the silicate uptake rate with an increase of DFe was observed in our experiments (see Fig. 4f). Hoffmann et al. (2007) investigated the elemental composition of *F. kerguelensis* and found no differences in the ratio of C:N:P regardless of the DFe of the medium. In addition, the ratio of C:N:P = 22:4:1 on average is far different from the Redfield ratio for both carbon and nitrogen against phosphorus, while the ratio of C:N = 5.5:1 is quite similar, implying a high accumulation of phosphorus in the diatom. Related to the mean uptake of nutrients, our results support preferential uptake of phosphorus, as ΔC:ΔN:ΔP:ΔSi is smaller than the RB ratio with respect to P in the media. To summarize, the results from our experiments indicate that uptake of N by *F. kerguelensis* could be enhanced with increasing iron concentration and vice versa for Si and P.

The ultimate goals of most iron experiments are not only to comprehend the ecological processes behind iron's triggering of the stimulation of the ecological system but also to estimate the uptake rate of carbon due to iron fertilization, the so-called iron efficacy (εFe) (Boyd et al. 2007; de Baar et al. 2005). In our experiments, we estimated εFe by defining the ratio of the DIC uptake rate per cell ($\eta C = \Delta DIC/\Delta Cell$) to the DFe uptake per cell ($\eta Fe = \Delta Fe/\Delta Cell$). Because of little variation in ηFe in -Fe and 0Fe media (Fig. 5e), we again employed the same method used to determine the ratios between the nutrients for the mean value from 3 different media and for the +Fe medium. εFe for the mean was estimated to be 44 000 mol mol^{-1} and that for the +Fe medium was 19 000 mol mol^{-1} (Table 3). Although the uncertainties of εFe for the mean value are greater than a factor of one, the 2.3-fold difference in εFe between these two cases leads us to suspect a decrease of carbon uptake efficiency with increasing DFe. This finding is significant in that εFe would not be proportional to the amount of iron added to the ocean. Of course, it will stimulate the diatom to grow, but the efficiency implies that *F. kerguelensis* could not digest all the dissolved iron added.

Nevertheless, these two values for εFe are larger than a εFe of ~5600 that was estimated based on the observations from the iron fertilization experiments in high-nutrient and low-chlorophyll oceans (de Baar et al. 2005). Providing that the loss ratio of iron loading in the ocean is 75% of the artificial iron fertilization (de Baar et al. 2008), a εFe of ~23 000 is still close to the lower limit of εFe by *F. kerguelensis* estimated in this experiment.

5. Summary and Conclusions

We investigated the response of one of the major diatom species in the Southern Ocean, *F. kerguelensis*, to iron enrichment in laboratory culture experiments. Its growth characteristics, μ_{max} and K_m, were 0.21 d^{-1} and 1.27 nM, respectively. The latter allowed us to derive a linear growth rate when the diatom grows in a linear manner. Its linear

growth rate was augmented with an initial DFe increase at the rate of 36(± 11) cells mL^{-1} d^{-1} for the increase of 10^{-15} molar DFe on a single cell basis, indicating that DFe indeed stimulated the growth of *F. kerguelensis*. Among the nutrients and trace metals analyzed, the uptake rate of nitrate and dissolved Fe and Mo by single cell appeared to increase with NDFe, while silicate and phosphate showed decreasing trends with NDFe increase. However, large uncertainties prevented us from drawing a firm conclusion and indicate a need for further study. For the first time, we monitored CO_2, CH_4, and N_2O in culture media, which allowed us to directly determine the carbon uptake rates for single growing cells and to examine direct emission or consumption of CH_4 and N_2O. The carbon uptake rate by single cells decreased with an NDFe increase, indicating that cell growth was too fast to keep up with digesting carbon at a high NDFe. This is fairly similar to silicate uptake. Combining the luxurious use of DFe, the iron efficacy (εFe) of carbon uptake by *F. kerguelensis* dwindled with a DFe increase, pointing to the inefficient use of iron at higher concentrations. The εFe value determined from the present experiments was 44 000 mol mol^{-1} on average, which is ~8-fold higher than the value estimated from artificial iron fertilization experiments (de Baar et al. 2005). Although the temporal trend for CH_4 during the culture experiments hinted at a consumption of ~0.1 fmol per cell on average during growth, large uncertainties indicate a need for further studies. N_2O was produced at lower NDFe levels, which switched to consumption at high NDFe levels. Our results clearly showed a facultative response of *F. kerguelensis* to the different DFe concentrations, and we suspect that this switching is related to the differential capacity for nitrous oxide reduction depending on the DFe concentration. These are the first experiments on the production or consumption of CH_4 and N_2O by a diatom species. Further studies are required to confirm these results and elucidate the mechanism underlying the results.

Acknowledgement

Financial support for this research was provided by Korean Polar Research Programs (PE11050, PE13410, PM13020, and PP14020).

References

Anderson MA, Morel FMM (1982) The influence of aqueous iron chemistry on the uptake of iron by the coastal diatom *Thalassiosira weissflogii*. Limnol Oceanogr **27**:789-813

Boyd P, Ellwood M (2010) The biogeochemical cycle of iron in the ocean. Nature Geosci **3**:675-682

Boyd PW, Jickells T, Law C, Blain S, Boyle E, Buesseler K, Coale K, Cullen J, de Baar H, Follows M (2007) Mesoscale iron enrichment experiments 1993-2005:Synthesis and future directions. Science **315**:612-617

Boyd PW, Watson AJ, Law CS, Abraham ER, Trull T, Murdoch R, Bakker DC, Bowie AR, Buesseler KO, Chang H, Charette MA, Croot PL, Downing K, Frew RD, Gall MP, Hadfield M, Hall J, Harvey M, Jameson G, La Roche J, Liddicoat M, Ling RD, Maldonado M, McKay R, Nodder S, Pickmere S, Pridmore R, Rintoul S, Safi K, Sutton P, Strzepek R, Tanneberger K, Turner S, Waite A, Zeldis J (2000) A mesoscale phytoplankton bloom in the polar Southern Ocean stimulated by iron fertilization. Nature **407**:695-702

Brand LE, Sunda WG, Guillard RR (1983) Limitation of marine phytoplankton reproductive rates by zinc, manganese, and iron. Limnol Oceanogr **28**:1182-1198

Brzezinski MA (1985) The Si:C:N ratio of marine diatoms: Interspecific variability and the effect of some environmental variables. J Phycol **21**:347-357

Buesseler KO, Andrews JE, Pike SM, Charette MA (2004) The effects of iron fertilization on carbon sequestration in the Southern Ocean. Science **304**:414-417

Coale KH, Johnson KS, Chavez FP, Buesseler KO, Barber RT, Brzezinski MA, Cochlan WP, Millero FJ, Falkowski PG, Bauer JE, Wanninkhof RH, Kudela RM, Altabet MA, Hales BE, Takahashi T, Landry MR, Badigare RR, Wang X, Chase Z, Strutton P, Friederich G, Gorbunov MY, Lance VP, Hilting AK, Hiscosk MR, Demarest M, Hiscock WT, Sullivan KF, Tanner SJ, Gordon RM, Hunter CN, Elrod VA, Fitzwater SE, Jones JL, Tozzi S, Koblizek M, Roberts AE, Hermdon J, Brewster J, Landizinsky N, Smith GJ, Cooper D, Timothy D, Brown SL, Selph KE, Sheridan CC, Twining BS, Johnson ZI (2004) Southern Ocean iron enrichment experiment:carbon cycling in high-and low-Si waters. Science **304**:408-414

de Baar HJ, Boyd PW, Coale KH, Landry MR, Tsuda A, Assmy P, Bakker DC, Brzezinski MA, Buesseler KO, Boye M, Croot PL, Gervais F, Gorbunov MY, Harrison PJ, Hiscock WT, Laan P, Lancelot C, Law CS, Lavasseur M, Marchetti A, Millero FJ, Nishioka J, Nojiri Y, van Oijen T, Riebesell U, Rijkenberg MJA, Saito H, Takeda S, Timmermans KR, Veldhuis M, Waite A, Wong CS (2005) Synthesis of iron fertilization experiments:From the Iron Age in the Age of Enlightenment. J Geophys Res-Oceans **110**:C09S16. doi:10.1029/2004JC002601

de Baar HJ, de Jong JT, Bakker DC, Löscher BM, Veth C, Bathmann U, Smetacek V (1995) Importance of iron for plankton blooms and carbon dioxide drawdown in the Southern Ocean. Nature **373**:412-415

de Baar HJW, Gerringa LJA, Laan P, Timmermans KR (2008) Efficiency of carbon removal per added iron in ocean iron fertilization. Mar Ecol-Prog Ser **364**:269-282

Doucette GJ, Harrison PJ (1990) Some effects of iron and nitrogen stress on the red tide dinoflagellate *Gymnodinium sanguineum*. Mar Ecol-Prog Ser **62**:293-306

Doucette GJ, Harrison PJ (1991) Aspects of iron and nitrogen nutrition in the red tide dinoflagellate *Gymnodinium sanguineum*. Mar Biol **110**:165-173

Elkins JW, Wofsy SC, McElroy MB, Kolb CE, Kaplan WA (1978) Aquatic sources and sinks for nitrous oxide. Nature **275**:603-606

Ferrón S, Ho DT, Johnson ZI, Huntley ME (2012) Air-water fluxes of N_2O and CH_4 during microalgae (*Staurosira* sp.) cultivation in an open raceway pond. Environ Sci Technol **46**:10842-10848

Fitzwater SE, Johnson KS, Gordon RM, Coale KH, Smith Jr WO (2000) Trace metal concentrations in the Ross Sea and their relationship with nutrients and phytoplankton growth. Deep-Sea Res II **47**:3159-3179

Florez-Leiva L, Tarifeño E, Cornejo M, Kiene R (2010) High production of nitrous oxide (N_2O), methane (CH_4) and dimethylsulphoniopropionate (DMSP) in a massive marine phytoplankton culture. Biogeosci Discuss **7**:6705-6723

Geider RJ, La Roche J (1994) The role of iron in phytoplankton photosynthesis, and the potential for iron-limitation of primary productivity in the sea. Photosynth Res **39**:275-301

Geider RJ, La Roche J, Greene RM, Olaizola M (1993) Response of the photosynthetic apparatus of *Phaeodactylum triocornutum* (Bacillariophyceae) to nitrate, phosphate, or iron starvation. J Phycol **29**:755-766

Gerringa LJA, de Baar HJW, Timmermans KR (2000) A comparison of iron limitation of phytoplankton in natural oceanic waters and laboratory media conditioned with EDTA. Mar Chem **68**:335-346

Granger J, Ward BB (2003) Accumulation of nitrogen oxides in copper-limited cultures of denitrifying bacteria. Limnol Oceanogr **48**:313-318

Guillard RR (1975) Culture of phytoplankton for feeding marine invertebrates. In: Culture of marine invertebrate animals. Springer US, pp 29-60

Hassler CS, Schoemann V, Nichols CM, Butler EC, Boyd PW (2011) Saccharides enhance iron bioavailability to Southern Ocean phytoplankton. P Natl Acad Sci **108**:1076-1081

Hiscock WT, Millero FJ (2005) Nutrient and carbon parameters during the Southern Ocean iron experiment (SOFeX). Deep-Sea Res I **52**:2086-2108

Ho TY, Quigg A, Finkel ZV, Milligan AJ, Wyman K, Falkowski PG, Morel FMM (2003) The elemental composition of some marine phytoplankton. J Phycol **39**:1145-1159

Hoffmann L, Peeken I, Lochte K (2007) Effects of iron on the elemental stoichiometry during EIFEX and in the diatoms *Fragilariopsis kerguelensis* and *Chaetoceros dichaeta*. Biogeosciences **4**:569-579

Hoogenhout H, Amesz J (1965) Growth rates of photosynthetic microorganisms in laboratory cultures. Archiv für Mikrobiologie **50**:10-25

Howarth RW, Cole JJ (1985) Molybdenum availability, nitrogen limitation, and phytoplankton growth in natural waters. Science **229**:653-655

Jickells T, An Z, Andersen KK, Baker A, Bergametti G, Brooks N, Cao J, Boyd P, Duce R, Hunter K (2005) Global iron connections between desert dust, ocean biogeochemistry, and climate. Science **308**:67-71

Lane TW, Morel FM (2000) A biological function for cadmium in marine diatoms. P Natl Acad Sci **97**:4627-4631

Laws EA (2013) Evaluation of in situ phytoplankton growth rates:A synthesis of data from varied approaches. Annu Rev Mar Sci **5**:247-268

Lewin J, Chen C (1971) Available iron:a limiting factor for marine phytoplankton. Limnol Oceanogr **16**:670-675

Loscher BM, de Baar HJW, de Jong JTM, Veth C, Dehairs F (1997) The distribution of Fe in the Antarctic circumpolar current. Deep-Sea Res **44**:143-187

Maldonado MT, Price NM (1996) Influence of N substrate on Fe requirements of marine centric diatoms. Mar Ecol-Prog Ser **141**:161-172

Marchetti A, Maldonado MT, Lane ES, Harrison PJ (2006) Iron requirements of the pennate diatom Pseudonitzschia:Comparison of oceanic (high-nitrate, low-chlorophyll waters) and coastal species. Limnol Oceanogr **51**:2092-2101

Marchetti A, Varela DE, Lance VP, Johnson Z, Palmucci M, Giordano M, Armbrust EV (2010) Iron and silicic acid effects on phytoplankton productivity, diversity, and chemical composition in the central equatorial Pacific Ocean. Limnol Oceanogr **55**:11-29

Martin JH (1990) Glacial-interglacial CO_2 change:The iron hypothesis. Paleoceanography **5**:1-13

Millero FJ (1998) Solubility of Fe (III) in seawater. Earth Planet Sci Lett **154**:323-329

Millero FJ, Yao W, Aicher J (1995) The speciation of Fe (II) and Fe (III) in natural waters. Mar Chem **50**:21-39

Monod J (1949) The growth of bacterial cultures. Annu Rev Microbiol **3**:371-394

Moore JK, Doney SC, Glover DM, Fung IY (2001) Iron cycling and nutrient-limitation patterns in surface waters of the World Ocean. Deep-Sea Res II **49**:463-507

Morel FMM, Price NM (2003) The biogeochemical cycles of trace metals in the oceans. Science **300**:944-947

Myhre G, Shindell D, Bréon F-M, Collins W, Fuglestvedt J, Huang J, Koch D, Lamarque J-F, Lee D, Mendoza B, Nakajima T, Robock A, Stephens G, Takemura T, Zhang H (2013) Anthropogenic and Natural Radiative Forcing. In:Stocker TF, Qin D, Plattner

G-K, Tignor M, Allen SK, Boschung J, Nauels A, Xia Y, Bex V, Midgley PM (eds) Climate Change 2013:the physical science basis contribution of working group I to the fifth assessment report of the Intergovernmental Panel on Climate Change. Cambridge University Press, Cambridge, UK and New York, pp 659-740

Nolting RF, Gerringa LJA, Swagerman MJW, Timmermans KR, de Baar HJW (1998) Fe (III) speciation in the high nutrient, low chlorophyll Pacific region of the Southern Ocean. Mar Chem **62**:335-352

Price NM, Ahner BA, Morel FMM (1994) The equatorial Pacific Ocean:Grazer-controlled phytoplankton populations in an iron-limited ecosystem. Limnol Oceanogr **39**:520-534

Redfield AC, Ketchum BH, Richards FA (1963) 2. The influence of organisms on the composition of sea-water. In: Hill NM (ed) The sea. Interscience, New York, pp 26-77

Rhee TS, Kettle AJ, Andreae MO (2009) Methane and nitrous oxide emissions from the ocean:A reassessment using basin-wide observations in the Atlantic. J Geophys Res-Atmos **114**:D12304. Doi: 10.1029/2008jd011662

Rhee TS, Park K, Hahm D, Shin HC, Lee S (2014) Impact of the southern ocean to the atmospheric CO_2, CH_4, and N_2O. In: 2014 SCAR Open Science Conference, Auckland, New Zealand, pp 383

Rue EL, Bruland KW (1995) Complexation of iron (III) by natural organic ligands in the Central North Pacific as determined by a new competitive ligand equilibration/adsorptive cathodic stripping voltammetric method. Mar Chem **50**:117-138

Sarmiento JL, Orr JC (1991) Three-dimensional simulations of the impact of Southern Ocean nutrient depletion on atmospheric CO_2 and ocean chemistry. Limnol Oceanogr **36**:1928-1950

Sarthou G, Timmermans KR, Blain S, Tréguer P (2005) Growth physiology and fate of diatoms in the ocean:A review. J Sea Res **53**:25-42

Smetacek V, Assmy P, Henjes J (2004) The role of grazing in structuring Southern Ocean pelagic ecosystems and biogeochemical cycles. Antarct Sci **16**:541-558

Sohrin Y, Urushihara S, Nakatsuka S, Kono T, Higo E, Minami T, Norisuye K, Umetani S (2008) Multielemental determination of GEOTRACES key trace metals in seawater by ICP-MS after preconcentration using an ethylenediaminetriacetic acid chelating resin. Anal Chem **80**:6267-6273

Stefels J, van Leeuwe MA (1998) Effects of iron and light stress on the biochemical composition of Antarctic *Phaeocystis* sp.(Prymnesiophyceae). I. Intracellular DMSP concentrations. J Phycol **34**:486-495

Sunda WG, Huntsman SA (1995) Iron uptake and growth limitation in oceanic and coastal phytoplankton. Mar Chem **50**:189-206

Sunda WG, Swift DG, Huntsman SA (1991) Low iron requirement for growth in oceanic phytoplankton. Nature **351**:55-57

Takeda S (1998) Influence of iron availability on nutrient consumption ratio of diatoms in oceanic waters. Nature **393**:774-777

Timmermans KR, Gerringa LJA, de Baar HJW, van der Wagt B, Veldhuis MJW, de Jong JTM, Croot PL, Boye M (2001) Growth rates of large and small Southern Ocean diatoms in relation to availability of iron in natural seawater. Limnol Oceanogr **46**:260-266

Timmermans KR, van der Wagt B (2010) Variability in cell size, nutrient depletion, and growth rates of the Southern Ocean diatom *Fragilariopsis kerguelensis (*Bacillariophyceae) after prolonged iron limitation. J Phycol **46**:497-506

Timmermans KR, van der Wagt B, de Baar HJ (2004) Growth rates, half-saturation constants, and silicate, nitrate, and phosphate depletion in relation to iron availability of four large, open-ocean diatoms from the Southern Ocean. Limnol Oceanogr **49**:2141-2151

Twining BS, Baines SB (2013) The trace metal composition of marine phytoplankton. Annu Rev Mar Sci **5**:191-215

UNESCO (1966) Second report of the Joint Panel on Oceanographic Tables and Standards. UNESCO technical papsers in marine science No. 4

van der Spoel S, Hallegraeff GM, van Soest RWM (1973) Notes on variation of diatoms and silicoflagellates in the South Atlantic Ocean. Netherlands J Sea Res **6**:518-541

van Leeuwe MA, Scharek R, de Baar HJW, de Jong JTM, Goeyens L (1997) Iron enrichment experiments in the Southern Ocean: physiological responses of plankton communities. Deep-Sea Res II **44**:189-207

van Oijen T, van Leeuwe MA, Granum E, Weissing FJ, Bellerby RGJ, Gieskes WWC, de Baar HJW (2004) Light rather than iron controls photosynthate production and allocation in Southern Ocean phytoplankton populations during austral autumn. J Plankton Res **26**:885-900

Wingenter OW, Haase KB, Strutton P, Friederich G, Meinardi S, Blake DR, Rowland FS (2004) Changing concentrations of CO, CH_4, C_5H_8, CH_3Br, CH_3I, and dimethyl sulfide during the Southern Ocean Iron Enrichment Experiments. P Natl Acad Sci **101**:8537-8541

Zielinski U, Gersonde R (1997) Diatom distribution in Southern Ocean surface sediments (Atlantic sector):implications for paleoenvironmental reconstructions. Palaeogeogr Palaeoclimatol Palaeoecol **129**:213-250

Appendix A. A simple model of dissolved iron chemistry in the culture media

We estimated ferric ion (Fe^{3+}) speciation in the media, provided that the medium was composed of the substances listed in Table A1. Then, stability constants for complex ions related to Fe^{3+} chemistry (Table A2) were applied to determine the fraction of speciation that is chelated to inorganic and organic ligands and EDTA (Millero et al. 1995; Millero 1998; Gerringa et al. 2000). Because we did not measure the concentrations of the organic ligands in the media, three cases for their total concentrations from the literature were applied; one is from open ocean waters (Millero 1998) and the others from the Pacific sector of the Southern Ocean (Nolting et al. 1998). The fraction of Fe^{3+} speciation is listed in Table A3. The EDTA-chelated fraction decreases with an increase in the organic concentration.

Table A1. Chemical composition of the medium relevant to iron chemistry

Ion*	Concentration (mol kg^{-1})	Ion	Concentration (mol kg^{-1})
Na^+	4.523E-01	H^+	1.00E-08
Mg^{2+}	5.093E-02	CO^{2+}	1.91E-10
Ca^{2+}	9.918E-03	Cu^{2+}	1.1E-09
K^+	9.845E-03	Mn^{2+}	3.82E-07
Cl^-	5.264E-01	Zn^{2+}	2.79E-08
SO_4^{2-}	2.723E-02	HCO_3^-	1.00E-03
		CO_3^{2-}	1.00E-04

*Major ions were calculated by the ratios to salinity of the culture media, 33.75 ‰, according to constant composition of seawater (UNESCO 1966) and the others are from measurements.

Table A2. Stability constants for the formation of Fe^{3+} complexes

Species	Log *K*	Reference*	Species	Log *K*	Reference*
$FeOH^{2+}$	-2.62	1	$MnCl^+$	0.02	2
$Fe(OH)_2^+$	-6.4	1	$MnCl_2$	-0.84	2
$Fe(OH)_3$	-12.5	1	$MnSO_4$	1.03	2
$Fe(OH)_4^-$	-21.8	1	$Mn(EDTA)^{2-}$	13.4	2
$FeCl^{2+}$	0.57	1	$Zn(OH)_2$	-17.2	2
$FeCl_2^+$	0.13	1	$ZnCO_3$	4.12	2
$FeSO_4^+$	2.58	1	$Zn(CO_3)_2^{2-}$	8.45	2
$Fe(SO_4)_2^-$	3.45	1	$ZnSO_4$	1.15	2
Fe(Org)	21	3	$Zn(EDTA)^{2-}$	14.1	2
$Fe(Org)_2$	22	3	Zn(OH)Cl	-8.07	2
$Fe(EDTA)^-$	24.3	2	$CoSO_4$	1.32	2
$Fe(OH)(EDTA)^{2-}$	18	2	$CoCl^+$	-0.09	2
$Fe(OH)_2(EDTA)^{3-}$	8.04	2	$Co(OH)_2$	-18.6	2
$H(EDTA)^{3-}$	8.78	2	$Co(EDTA)^{2-}$	15.7	2
$H_2(EDTA)^{2-}$	14.2	2	$Cu(OH)_2$	-14	2
$H_3(EDTA)^-$	16.2	2	$CuCO_3$	5.55	2
$H_4(EDTA)$	18	2	$Cu(CO_3)_2^{2-}$	8.65	2
$Na(EDTA)^{3-}$	1.76	2	$Cu(EDTA)^{2-}$	16.4	2
$Ca(EDTA)^{2-}$	10.1	2			
$Mg(EDTA)^{2-}$	8.14	2			
$K(EDTA)^{3-}$	0.7	2			

*Reference: 1; Millero et al. (1995), 2;Gerringa et al. (2000), 3;Millero (1998)

Table A3. Fraction of Fe^{3+} speciation

Organic concentration (nM)	Inorganic ligand (%)	Organic ligand (%)	EDTA (%)	Reference*
0.17	1.5	64.4	34.1	1
2.2	0.17	95.9	3.92	2
12.3	0.03	99.2	0.73	2

*Reference: 1;Millero (1998), 2;Nolting et al. (1998)